Skid Prevention for EVs based on the Emulation of Torque Characteristics of Separately-wound DC Motor

Shinya Kodama
Department of Electrical Engineering
University of Tokyo
Email: kodama@horilab.iis.u-tokyo.ac.jp

Lianbing Li
Department of Electrical Engineering
University of Tokyo
Email: lilianbing@horilab.iis.u-tokyo.ac.jp

Yoichi Hori
Institute of Industrial Science
University of Tokyo
Email: hori@iis.u-tokyo.ac.jp

***Abstract*— It is well-known that the separately-wound DC motor has effective torque (current) reduction characteristics in response to rapid increase of the rotational speed of the motor. This characteristics has been utilized in adhesion control of electric locomotives with DC motor. In this paper, how to realize a new skid prevention method for EVs utilizing this characteristics is mentioned. In order to compensate for Back-EMF, disturbance observer is introduced. By selecting the time constant or observer gain properly, the torque (current) reduction characteristics can be adjusted freely in some range. The experimental results of the hardware skid simulator utilizing Motor-Generator setup verified the effectiveness of our proposed method.**

I. Introduction

In recent years, the Electric Vehicle (EV) has attracted considerable interests as one of hopeful solutions for solving environmental and energy problems.

The advantages of EVs that comes up first are high efficiency and low pollution. The merits of the EVs, however, such as fast and precise output torque and so on have not been developed by present. The output torque of the motor can be controlled to follow its reference value accurately, with a relatively short time constant of 1[ms] and much less dead time. There are still have many challenges and chances in the research of high-performance EV[1], [2], [3].

As an excellent example making use of fast response of EVs, the separately-wound DC motor with the torque (current) reduction characteristics is researched in this paper to develop a new skid prevention method between the EV and the road[4].

II. Skid Prevention based on Torque (Current) Reduction Characteristics of Separately-wound DC Motor

A. Motion of Vehicle

In this paper, the running state of an EV driven by separately-wound DC motor is researched with simulations and experimentations when the road surface is rapidly varied.

1) Dynamic Equations of Vehicle: Suppose that the time constant, the rolling resistance and the wind drag force are very small. The forces effecting on the vehicle are

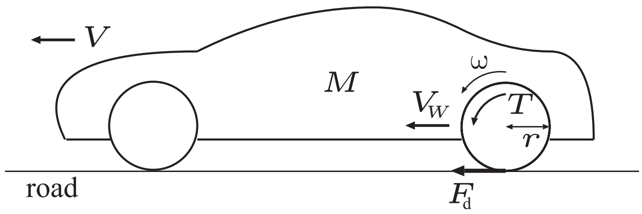

Fig. 1. The motion of vehicle.

shown in Fig.1, and the dynamic equations are expressed in (1) - (3).

$$\omega = \frac{1}{Js}(T - rF_d) \quad (1)$$

$$V = \frac{1}{Ms}F_d \quad (2)$$

$$V_W = r\omega \quad (3)$$

Where ω is the rotational speed of the wheel (motor), V is the speed of the vehicle, V_W is the speed of the wheel, F_d is the driving force, T is the driving torque of the motor and s is the Laplace operator. J is the inertia moment of all the rotating parts of the EV, r is the radius of the tire and M is the mass of the EV.

Equation (1) is the motion equation of the wheel, and the wheel is effected by the torque of the motor and the reaction force from the road. Equation (2) is the motion equation of the chassis.

2) Adhesion Characteristics of Tire and Road: The adhesion characteristics of tire and road can be expressed by the concept of slip ratio. Slip ratio λ is defined in the following equations utilizing V, V_W,

$$\lambda = \frac{V_W - V}{V_W} \quad \text{(Driving)} \quad (4)$$

$$\lambda = -\frac{V - V_W}{V} \quad \text{(Braking)} \quad (5)$$

Utilizing slip ratio λ, the relationship of the slip ratio and the friction coefficient μ between the tire and the road can be approximated and described, for example, by (6), which is called $\mu - \lambda$ curve (function).

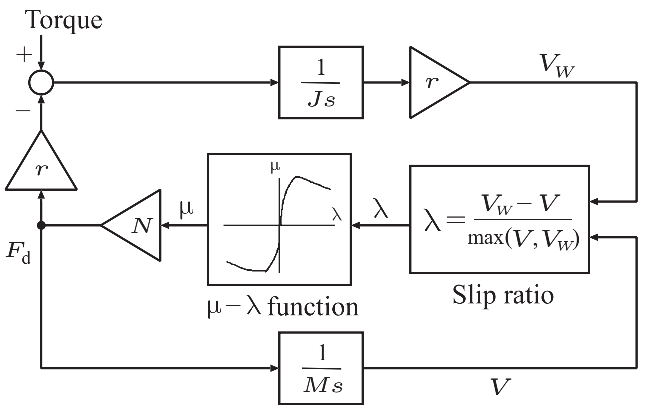

Fig. 2. The block diagram of the one-wheel vehicle model.

$$
\begin{aligned}
\mu &= -1.05k\{\exp(-45\lambda) - \exp(-0.45\lambda)\} \quad \text{(Driving)} \\
\mu &= 1.1k\{\exp(35\lambda) - \exp(0.35\lambda)\} \quad \text{(Braking)}
\end{aligned} \tag{6}
$$

Where k is the parameter of the road status, and takes the following values, for example,

$$
\begin{aligned}
k &= 1 \quad \text{(Dry road)} \\
k &= 0.2 \quad \text{(Icy road)}
\end{aligned} \tag{7}
$$

After having achieved the friction coefficient μ from slip ratio λ utilizing $\mu - \lambda$ curve, the driving force F_d can be calculated by (8).

$$F_d = \mu(\lambda)N \tag{8}$$

Where N is the normal component of reaction effecting on tires.

The model of the one-wheel EV can be shown in Fig.2.

B. The Skid Prevention Scheme utilizing Back-EMF

The block diagram of the EV system installed separately-wound DC motor is shown in Fig.3(a). G^{-1} in Fig.3(a) is the inverse function of the transfer function from the voltage command v^* to the current i. It is utilized to acquire the voltage command v^*.

Suppose that the vehicle is running from the dry road to the icy road, and the surface of the icy road is very smooth, so that the friction between the tire and the road is rapidly reduced. At the same time the motor of the EV is still keeping the driving torque as before, then the wheel will skid on the icy road quickly.

If the torque (current) reduction characteristics of the separately-wound DC motor, however, can be activated, the skid phenomenon will be restrained. Though the speed of the wheel quickly increases, the back-EMF that is proportional with the rotational speed of the wheel will increase at the same time to decrease the acceleration of the wheel. This is the scheme of the skid prevention utilizing the torque (current) reduction characteristics of separately-wound DC motor.

The advantage of this method is that the complicated calculation is not necessary and the torque (current) can be decreased quickly.

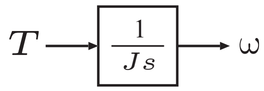

Fig. 4. The relation between the torque and the wheel speed.

Skid phenomenon is simulated utilizing the EV system as shown in Figs.2 and 3(a). The simulation is started at t = 0[s]. At t = 1[s], the EV starts to accelerate in the dry road, and at t = 6[s] it enters the icy road. The parameters of the EV system are utilized by "UOT March I" which is the experimental EV of our laboratory.

The simulation results are shown in Fig.3. For the sake of comparison, the curves controlled by FB current controller and ones with FF controller are shown in the same figures. The curve with FF current control in Fig.3(b) shows the torque reduction characteristics. As a result, the skid is restrained as shown in Figs.3(c) - 3(e).

C. The Emulation of the Vehicle Model with regarding it as an Inertia Term

Following (9) is derived from (1) - (4)[1].

$$\frac{\omega}{T} = \frac{1}{\{J + r^2 M(1-\lambda)\}s} \tag{9}$$

Regarding the denominator in this (9) as Js, the relationship between the torque and the rotational speed of the wheel is shown in Fig.4. Slip ratio λ is increased, since the difference between the rotational speed of the wheel and the vehicle speed becomes larger if the vehicle skids when driving. Therefore skid can be regarded as the phenomenon that J is decreased.

Thus in this paper the phenomenon that the inertia moment is decreased $1/3$ times as large as before can be regarded as the outbreak of skid on the EV. The inertia moment of the loading motor seen from the driving motor is decreased $1/3$ times as large as before in Chap.IV. The vehicle model is regarded as an inertia term from here on.

III. Adjustment of Skid Prevention Characteristics with Disturbance Observer

In previous section the torque (current) reduction characteristics is analyzed. In this chapter, this characteristics will be tried to adjust.

There is a possibility the characteristics of the torque (current) reduction has influence on the safety and ride quality of the EVs. That's because the range of the torque (current) reduction is expected to be adjustable freely. In fact the torque (current) reduction, however, depends on the physical parameters of the motor such as the reactance L and so on. The disturbance observer is designed to adjust the driving torque in order to complete this option without changing the installed motor itself in EV.

Skid prevention is simulated utilizing parameters of Motor-Generator setup, which will be gone into detail in Chap.IV.

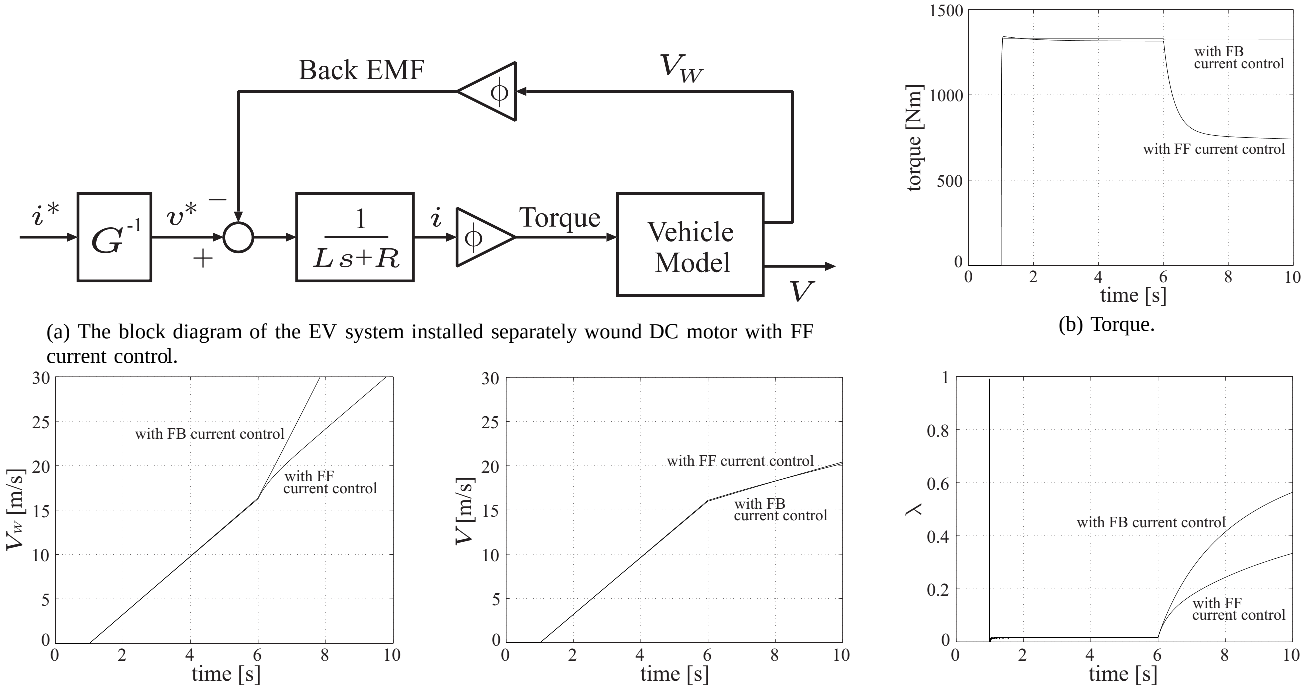

(a) The block diagram of the EV system installed separately wound DC motor with FF current control.

(b) Torque.

(c) Wheel speed.

(d) Vehicle speed.

(e) Slip ratio.

Fig. 3. The block diagram of the EV system and the simulation results of the skid phenomenon with utilizing parameters of EV (UOT March I). (The vehicle skids at t = 6[s] in the simulation.)

A. Adjustment of Torque (Current) Reduction Characteristics with Time Constant τ

1) Effectiveness of Adjustment with Time Constant τ: Regarding back-EMF as the disturbance on the DC motor, the block diagram with the disturbance observer is described as Fig.5(a). The vehicle model in this figure means the inertia term $1/Js$ as already mentioned.

If the time constant τ is much smaller, back-EMF is completely compensated and the disturbance does not act upon the current of the motor. On the contrary, if the time constant τ becomes larger, the response speed which keeps down the disturbance becomes slowly and the disturbance has much effect on the current of the motor in consequence. Thus adjusting the time constant τ, it is proved that effect of back-EMF on the current of the motor can be controlled.

2) Analysis with Simulation: Depending on the conception of the previous section, the results of simulation changing the time constant τ from 0.001 to 10 are shown Fig.5, where the compensation gain K is 1.

Fig.5(b) shows that the time constant τ changes the torque (current) reduction characteristics. The larger the time constant τ is, the larger the current reduction is when the vehicle skids. As a result this characteristics prevents the rotational speed of the motor from rapid increase shown in Fig.5(c). Since back-EMF, namely it is the disturbance, is, and yet at the same time, compensated when the time constant τ is small enough, the current of the motor is equaled to the current command and the rotational speed of the motor rapidly increases when the vehicle skids.

Next, the change of the torque (current) reduction characteristics with the time constant τ is quantitatively considered.

In Fig.5(a) the transfer function from the voltage command v^* to the current i is shown in (10).

$$G(s)(=\frac{i}{v^*})=\frac{J\tau s^2+Js}{JL\tau s^3+J(L+R\tau)s^2+(JR+\phi^2\tau)s+\phi^2(-K+1)} \quad (10)$$

G^{-1} becomes (11) if regarding J which is constant value J_n when the vehicle is in steady-state driving.

$$G^{-1}(s)=\frac{J_nL\tau s^3+J_n(L+R\tau)s^2+(J_nR+\phi^2\tau)s+\phi^2(-K+1)}{J_n\tau s^2+J_ns} \quad (11)$$

Utilizing (10) and (11), the transfer function from the current command i^* to the current of the motor i is shown in (12).

$$\frac{i(s)}{i^*(s)}=\frac{J_nL\tau s^3+J_n(L+R\tau)s^2+(J_nR+\phi^2\tau)s+\phi^2(-K+1)}{JL\tau s^3+J(L+R\tau)s^2+(JR+\phi^2\tau)s+\phi^2(-K+1)}\frac{J}{J_n} \quad (12)$$

The value of (12) is 1 because J is equal to J_n when the vehicle is in steady-state driving. Drivers can, that is to say, control the longitudinal motion of the vehicle with abandon because the vehicle is braking or driving by the current of the motor which arbitrary current command itself becomes when the vehicle is in steady-state driving.

In the second place behaviors of the vehicle are analyzed when the vehicle skids. The inertia moment seen by the motor becomes lighter when the wheel skids than when the vehicle is in steady-state driving. In this part, the skid phenomenon is analyzed with regarding that as the phenomenon that the inertia moment J rapidly decreases. Giving the compensation gain K is 1, the final value of the step response on (12) is shown in (14) utilizing the Final

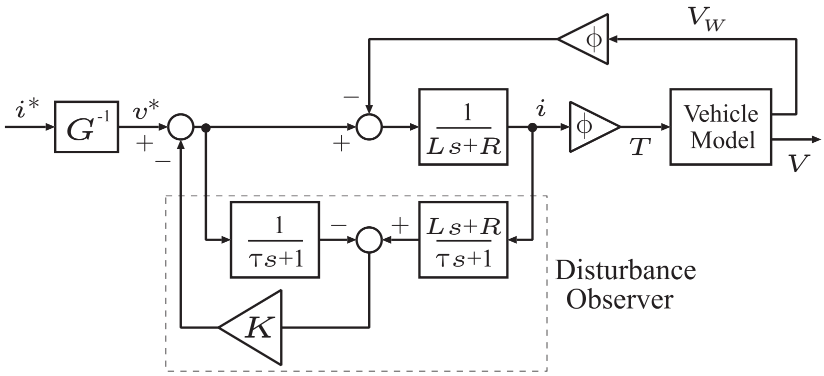

(a) The block diagram of the disturbance observer and the EV system installed separately wound DC motor with FF current control.

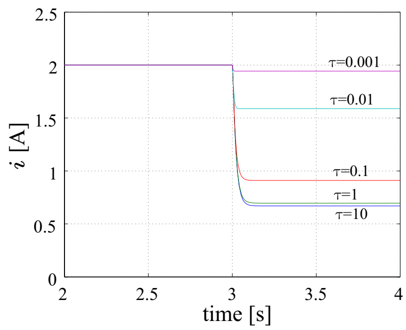

(b) The current of the motor. (The time constant τ is turned.)

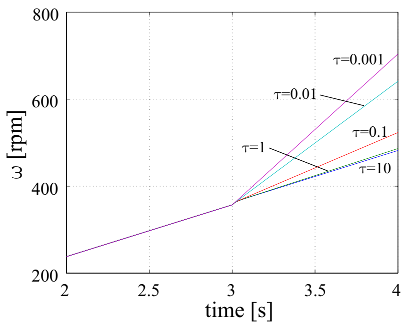

(c) The rotational speed of the motor. (The time constant τ is turned.)

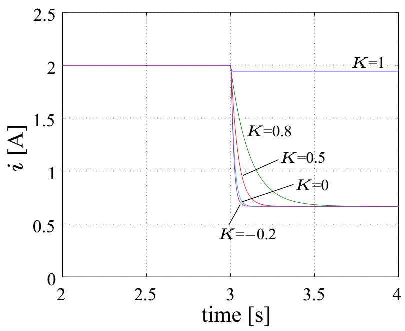

(d) The current of the motor. (The gain K is turned.)

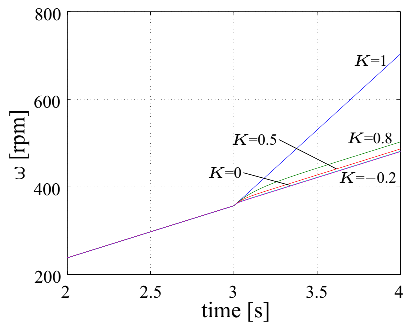

(e) The rotational speed of the motor. (The gain K is turned.)

Fig. 5. The block diagram of the disturbance observer and the simulation results of the skid phenomenon with utilizing parameters of MG setup. (The current command i^* = 2[A], the motor skids at t = 3[s] in the simulation.)

Value Theorem shown in (13), where $r(t)$ means the step input.

$$\lim_{t\to\infty} \frac{i(t)}{i^*(t)} r(t) = \lim_{s\to 0} s \frac{i(s)}{i^*(s)} \frac{1}{s} \tag{13}$$

$$= \frac{J_n R + \phi^2 \tau}{JR + \phi^2 \tau} \frac{J}{J_n} \tag{14}$$

Equation (14) shows that the change of the inertia moment J of the transfer function from the current command i^* to the real current i depends on the time constant τ. The torque (current) reduction characteristics does not appear since the value of (14) is always 1 and the current command directly becomes the real current of the motor if the time constant τ is small enough. On the contrary, the value of (14) becomes J/J_n and the motor current becomes J/J_n times larger than the current command if the time constant τ is large enough. This rapid decrease of the current is the phenomenon called the torque (current) reduction characteristics.

In conclusion, it is proved that the torque (current) reduction characteristics can be freely adjusted by the time constant τ when the vehicle skids. It takes a little time to reduce the torque (current), even if this method is superior to the other. Therefore, the problem of this method is that the rotational speed of the motor rapidly rises once, seen in Fig.5(c), even if the time constant τ is large enough.

B. Adjustment of Torque (Current) Reduction Characteristics with Gain K

1) Effectiveness of Adjustment with Gain K: In this section adjustment of the torque (current) reduction characteristics with changing gain K is considered in view of the problem that it takes a little longer time for proposed method until the torque (current) reduces. Equation (12) is the secondary delay system under the circumstances that gain is fixed $K = 1$. Equation (12) becomes, however, the 3rd delay system on the condition that gain is $K \neq 1$ and the pole equation becomes complicated. Routh's Stability Criterion shows the condition that if K satisfies following (15) the pole equation can be kept stable.

$$1 - \frac{(L + R\tau)(JR + \phi^2 \tau)}{L\tau\phi^2} < K < 1 \tag{15}$$

That's because the time response of (12) can be freely adjusted by changing gain K only when K satisfies (15). It is possible, in other words, to cut down the delay of the time response by means of adjusting gain K.

2) Analysis with Simulation: When the time constant τ is fixed $\tau = 0.001$ and gain K is enlarged from 1 to the negative direction, the torque (current) reduction characteristics when the vehicle skids is simulated. Results are shown in Fig.5.

Fig.5(d) shows that the torque (current) reduction is quickened as gain K is enlarged to the negative direction when the vehicle skids. Fig.5(e) shows that the larger K is

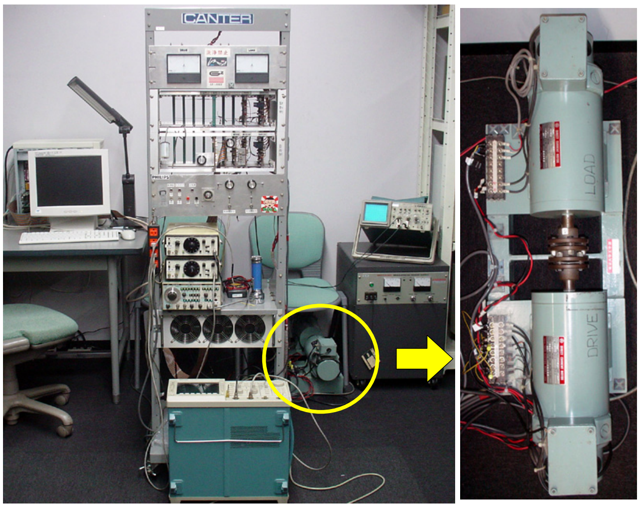

Fig. 6. Motor-Generator setup.

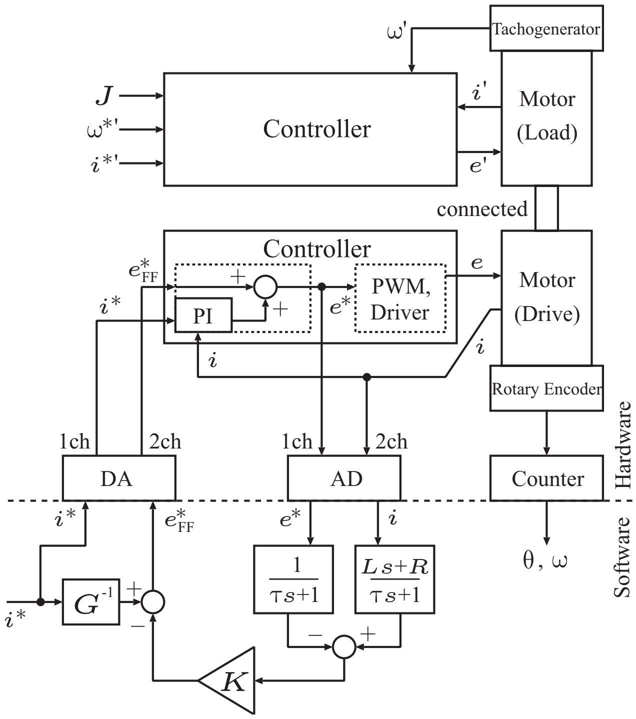

Fig. 7. The block diagram of the control system of MG setup. (The PI controller is not utilized when the FF current controller is utilized.)

to the negative direction, the more the rotational speed of the motor is prevented from rapid increase.

In conclusion, it is proved that the final value of the torque when the vehicle skids is decided by the time constant of the disturbance observer and the speed of the torque (current) reduction by gain. The most appropriate combination of both the time constant and gain in view of the destination should be considered and the torque (current) reduction characteristics be decided in order to utilize characteristics of separately-wound DC motor which prevents vehicle from skidding effectively.

IV. Experimentation of Motor-Generator Setup

A. Outline of Experimentations

Motor-Generator setup is shown in Fig.6 and the sketch of control system is shown in Fig.7. The torque (current) reduction when the vehicle skids and the circumstances that the disturbance observer adjusts torque reduction characteristics is observed utilizing Motor-Generator setup, where the shafts of two motors (the driving motor and the loading motor), are interconnected. The loading motor is controlled by the only hardware controller boards and the inertia moment of the loading motor seen from the driving motor can be controlled. The driving motor is controlled by the hardware controller and software one. That is to say, PI controller, driver of the motor and so on consist of hardware, but disturbance observer and G^{-1} filter are designed as software controller. DA, AD, counter boards act as a bridge between hardware and software. The sampling time of the software controller is 1[ms]. The current command i^* = 2[A], the inertia moment is rapidly decreases at about t = 3[s], which means the vehicle begins to skid.

B. Confirmation of Torque (Current) Reduction Characteristics

The experimental test was performed in order to confirm the torque (current) reduction characteristics shown in Chap.II. The current of the motor and the rotational speed are observed at the accelerated speed when the vehicle skids both in the case where pre-filter G^{-1} shown in Fig.3(a) is only added to separately-wound DC motor and in the case where the motor is controlled only by the current controller. Results are shown in Fig.8.

The inertia moment of the motor which is simulated the skid phenomenon decreases rapidly at about t = 3[s]. Fig.8(a) shows that the current of the motor reduces when the inertia moment decreases if only pre-filter is being utilized. Therefore, the rotational speed of the motor is prevented from rapid increase in Fig.8(b). In contrast, the rotational speed of the motor is, as a result, rapidly increased since the current of the motor is held constant when utilizing the FB current controller even if the inertia moment decreases.

C. Adjustment of Torque (Current) Reduction Characteristics utilizing Disturbance Observer

Then the experimental tests with the torque (current) reduction characteristics adjusting was performed utilizing the disturbance observer. Five ways where the gain is fixed $K = 1$ and the time constant τ is changed from 0.001 to 10 are tried. Each experimental results are shown in Fig.8. Fig.8(c) shows that the larger the time constant τ is, the larger the current reduction becomes. As a result the rotational speed of the motor is prevented from rapid increase as shown in Fig.8(d).

Finally results of experimental tests when the time constant is fixed $\tau = 0.001$ and gain K of the disturbance observer is changed are shown in Fig.8. Fig.8(e) shows that the larger gain K becomes to the negative direction, the more rapidly the torque (current) reduces. The larger gain is

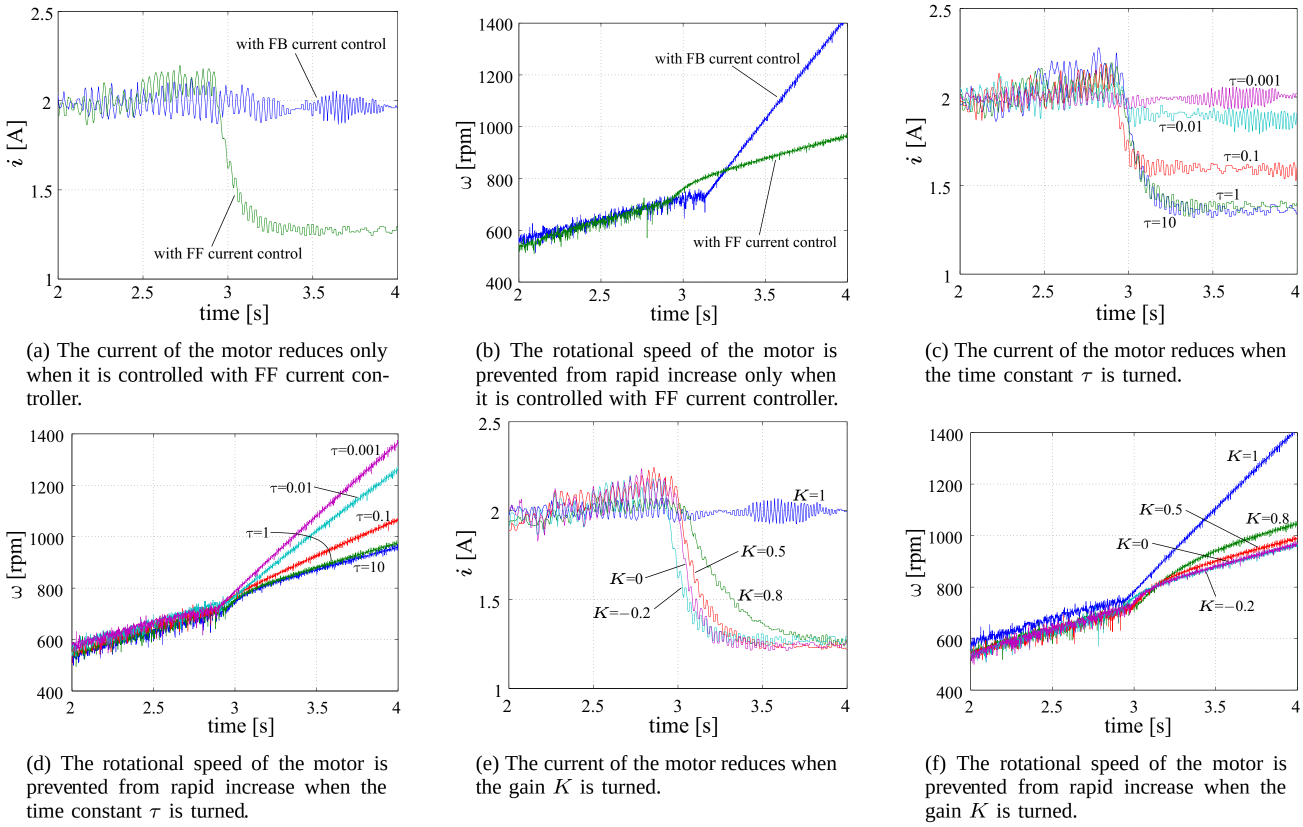

(a) The current of the motor reduces only when it is controlled with FF current controller.

(b) The rotational speed of the motor is prevented from rapid increase only when it is controlled with FF current controller.

(c) The current of the motor reduces when the time constant τ is turned.

(d) The rotational speed of the motor is prevented from rapid increase when the time constant τ is turned.

(e) The current of the motor reduces when the gain K is turned.

(f) The rotational speed of the motor is prevented from rapid increase when the gain K is turned.

Fig. 8. The experimental results of the skid phenomenon with utilizing MG setup. (The torque (current) reduction characteristics can be confirmed. The current command $i^* = 2$[A], the motor skids at about $t = 3$[s].)

to the negative direction, as a result, the more the rotational speed of the motor is prevented from rapid increase after the inertia moment decreased as shown in Fig.8(f). These results are almost same to simulation ones.

It is demonstrated, in consequence, that the torque (current) reduction characteristics of separately-wound DC motor can be freely adjusted with changing the time constant and gain of the disturbance observer. Quickly response may be able to become a great advantage because of utilizing innate characteristics of motor, though proposed method cannot completely prevent EVs from skidding. Our proposed method could guarantee beneficial effects on skid prevention for EVs if it is combined with other motor control methods.

V. Conclusion

The fundamental principle of the adhesion control is that the large torque (current) reduction characteristics is shown in a micro time scale, when the wheel skids slightly, but the characteristics which outputs the defined torque is shown in a macroscopic time scale. This is the very characteristics of the separately-wound DC motor driven by the voltage supply.

The AC motor made of permanent magnet is the most appreciated and most commonly utilized for EVs at the present day and it is controlled by the high-performance current controller. It is little-known that, however, this current control is the worst in terms of the adhesion performance, so the existing control methods are premised on the current control.

A skid prevention method for EVs was developed that was focused on this torque (current) reduction characteristics in this paper. It would not be an exaggeration to say that the significant possibility that effects on skid prevention was found out. Now a new electric vehicle driven by the BLDC motor to put this proposed method into practice is in the process of production.

If the development of our studies comes to be utilized widely, needless to say, the risk of skid becomes dramatically small enough. It also can contribute greatly to safety improvement of the vehicle utilizing the advanced attitude control system even if driving on the skiddy road and improve infinitely energy efficiency which is a critical problem for EVs utilizing lower-loss tires.

References

[1] Y. Hori, "Traction Control of Electric Vehicle: Basic Experimental Results Using the Test EV UOT Electric March," *IEEE Trans. on Industry Applications*, Vol. 34, No. 5, pp.1131–1138, 1998.

[2] S. Sakai and Y. Hori, "Advantage of Electric Motor for Anti Skid Control of Electric Vehicle," *EPE Journal*, Vol.11, No.4, pp.26–32, 2001.

[3] S. Matsugaura, et al., "Evaluation of Performances for the In-Wheel Drive System for the New Concept Electric Vehicle KAZ," in *Proc. EVS19*, Pusan, Korea, 2002.

[4] T. Miyamoto and Y. Hori, "Adhesion Control of EV Based on Disturbance Observer," *IEE of Japan Technical Meeting Record, IIC-00-9*, pp.49–54, 2000. [In Japanese]